Biochemical and Biophysical Research Communications xxx (xxxx) xxx

Contents lists available at ScienceDirect

Biochemical and Biophysical Research Communications

journal homepage: www.elsevier.com/locate/ybbrc

Structural basis for stereospecificity to D-amino acid of glycine oxidase from *Bacillus cereus* ATCC 14579

Jihye Seok [a, b], Yeo-Jin Kim [a], Il-Kwon Kim [b], Kyung-Jin Kim [a, b, *]

[a] School of Life Sciences, KNU Creative BioResearch Group, Kyungpook National University, Daehak-ro 80, Buk-ku, Daegu, 41566, Republic of Korea
[b] KNU Institute for Microorganisms, Kyungpook National University, Daehak-ro 80, Buk-ku, Daegu, 41566, Republic of Korea

ARTICLE INFO

Article history:
Received 20 September 2020
Accepted 22 September 2020
Available online xxx

Keywords:
Glycine oxidase
Bacillus cereus
D-amino acid
Stereochemistry
Glyphosate

ABSTRACT

Glycine oxidase (GO) is an enzyme that catalyzes the oxidation of the primary and secondary amines of various chemicals, including glycine, and the enzyme has been applied in a variety of fields, such as biosensor and genetically modified glyphosate resistance plants. Here, we report that the gene product of *BC0747* from *Bacillus cereus* (*Bc*GO) shows oxidase activity for glycine and small D-amino acids, such as D-proline and D-alanine. We also determined the crystal structure of *Bc*GO complexed with the FAD cofactor at a 2.36 Å resolution and revealed how the cofactor binds to the deep pocket of the enzyme. We performed the molecular docking calculation of the glycine substrate to the *Bc*GO structure and identified how the carboxyl- and amine-groups of the D-amino acid are stabilized at the substrate binding site. Structural analysis of *Bc*GO also provided information on the structural basis for the stereospecificity of the enzyme to D-amino acids. In addition, we placed the glyphosate molecule, a plant herbicide, at the substrate binding site, and explained how the mutation of Gly51 to arginine enhances enzyme activity.

1. Introduction

Glycine oxidase (GO, EC 1.4.3.19) is an enzyme that catalyzes the oxidation of the primary and secondary amines of various chemicals, including glycine. Since GO from *Bacillus subtilis* (*Bs*GO) was first cloned in 1998 [1], GOs have been reported from several microorganisms, including *Pseudomonas putida* KT2440 [2], *Geobacillus kaustophilus* [3], and *B. licheniformis* [4]. GO is a flavoprotein that contains flavin adenine dinucleotide (FAD) as a non-covalent cofactor. Together with D-amino acid oxidase (DAAO, EC 1.4.3.3) and sarcosine oxidase (SOX, EC 1.5.3.1), GO is a member of the amine oxidase class of flavoproteins. GOs from *P. putida* KT2440 and *G. kaustophilus* (*Gk*GO) have been reported to have enzymatic activity on various D-form compounds, such as D-norvaline, D-valine, D-arginine, D-proline, D-methionine, and glycine, producing the corresponding α-keto acids, ammonia/amine, and hydrogen peroxide [2,3,5].

GO catalyzes two consecutive reactions to produce glyoxylate from glycine; dehydration of glycine to 2-iminoacetate, and hydration of 2-iminoacetate to glyoxylate [6] (Fig. 1A). In this process, FAD undergoes changes to its oxidation and reduction status producing hydrogen peroxide [7]. GO is also known as ThiO and is involved in the biosynthetic pathway of the thiazole moiety of thiamine pyrophosphate (vitamin B1) in *B. subtilis*. The thiazole moiety is synthesized from glyceraldehyde-3-phosphate, pyruvate, and glycine, and the biosynthesis involves several enzymes, including ThiI, ThiF, ThiS, ThiG, ThiO, and TenI [8,9]. In the synthesis of the thiazole moiety, instead of converting to glyoxylate, the 2-iminoacetate molecule produced by the first oxidation reaction of ThiO is combined with ThiS-OSH via the action of ThiG [8]. GO has been applied in various fields, specifically through the utilization of its broad substrate specificity and stereospecificity, which means GO specifically targets stereoisomeric reactants. For example, *Bs*GO has been used as a biosensor to detect small achiral amino acids such as glycine [10]; GO has also been employed to confer resistance to glyphosate herbicide by oxidizing glyphosate, which inhibits 5-enolpyruvylshikimate-3-phosphate synthase of the shikimate pathway in plants [11–14].

GO from *B. cereus* (*Bc*GO) was first reported in the strain HYC-7 in 2013 [14]. In particular, several mutation experiments were reported to increase the glyphosate affinity of *Bc*GO 10 to 160 times [14,15]. *Bacillus cereus* ATCC 14579 is a rod-shaped, gram-positive strain, and its whole genome sequence was published in 2003 [16].

* Corresponding author. Kyungpook National University, School of Life Sciences, Structural and Molecular Biology Laboratory, Room 409, Biology building, Kyungpook National University, Daehak-ro 80, Buk-ku, Daegu, Republic of Korea.
E-mail address: kkim@knu.ac.kr (K.-J. Kim).

https://doi.org/10.1016/j.bbrc.2020.09.093
0006-291X/

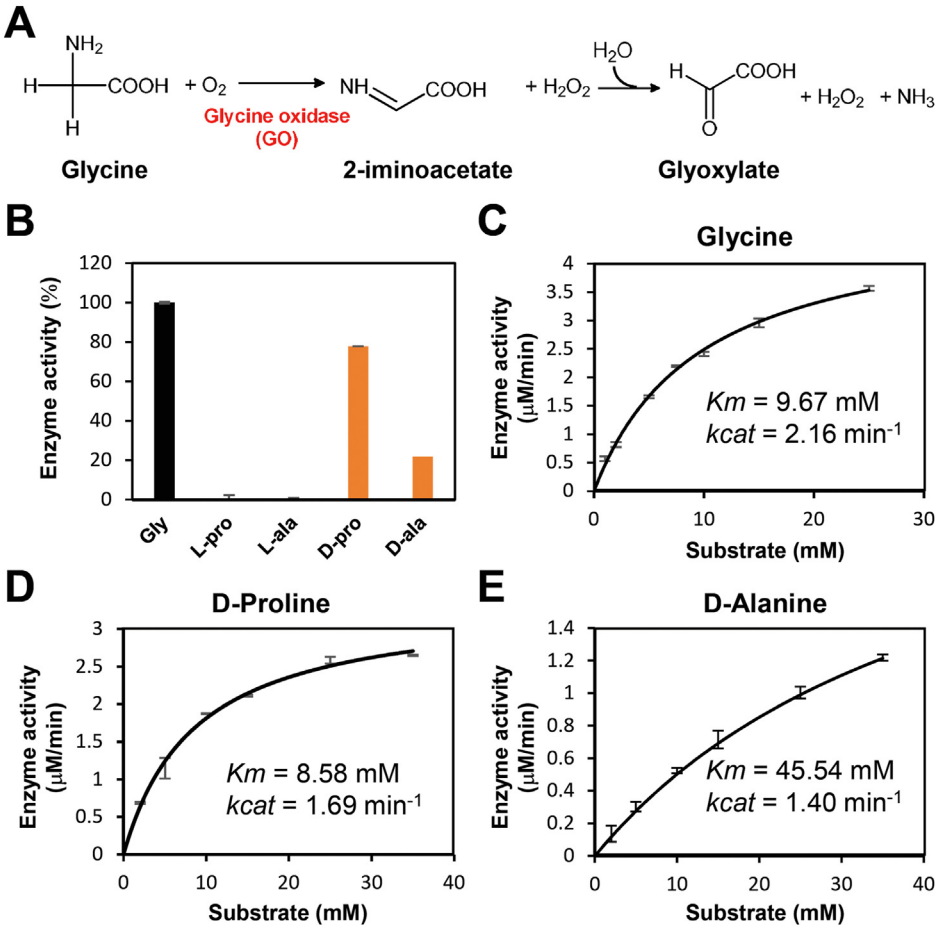

Fig. 1. Glycine oxidase reaction and kinetic properties of *Bc*GO. (A) Reaction of glycine oxidase. (B) Relative activities of *Bc*GO with various small amino acid as substrates. The experiments are conducted in triplicate. (C)(D)(E) Enzyme kinetic analysis of *Bc*GO. Reaction velocity was plotted versus each substrate concentration based on the Michaelis-Menten equation. Various concentrations of glycine (2.5–25 mM, C), D-proline (5–35 mM, D), and D-alanine (2.5mM–35mM, E) were used.

When we analyzed the genomic information for *B. cereus* in the Kyoto Encyclopedia of Genes and Genomes (KEGG) [17], the strain was found to contain the *BC0747* gene annotated as a glycine oxidase (*Bc*GO) within the operon for thiamine-moiety biosynthesis. Here, we report on the results of our biochemical and kinetic investigation of *Bc*GO, which revealed that *Bc*GO is stereospecific for D-amino acids. We also report on the crystal structure of *Bc*GO complexed with the FAD cofactor. Most importantly, we provide the structural basis for the substrate binding mode of D-amino acids and the stereospecificity of *Bc*GO for D-amino acids.

2. Materials and methods

2.1. Preparation of BcGO

The *Bc*GO coding gene was amplified by polymerase chain reaction (PCR) using the chromosome from *Bacillus cereus* ATCC 14579. The PCR product was digested by restriction enzyme, and cloned into the pET30a (Novagen) expression vector. The pET30a:*Bc*GO was transformed into an *Escherichia coli* BL21 (DE3)-T1R strain, which was grown in 1 L of LB medium containing kanamycin (50 mg L^{-1}) at 37 °C. When OD600 reaches to an 0.6, the gene expression was induced by the addition of 1.0 mM isopropyl 1-thio-β-D-galactopyranoside (IPTG), and the culture medium was further maintained at 18 °C for 20 h. The culture medium was harvested by centrifugation at 4000 g and 4 °C for 20 min. The cell pellet was resuspended in 40 mM Tris-HCl, pH 8 and disrupted by ultrasonication. The cell debris was removed through centrifugation at 13,500 g and 4 °C for 30 min and the lysate was applied to a Ni-NTA agarose column (QIAGEN). After washing with buffer containing 25 mM imidazole, the bound proteins were eluted with 300 mM imidazole. Finally, a trace amount of contaminants was removed by size exclusion chromatography using a HiPrep 26/60 Sephacryl S-300 HR column (GE Healthcare Life Sciences).

2.2. Protein activity assay

For activity assay of *Bc*GO, we measured H_2O_2 produced as a product when the substrate is oxidase by GO through a coupled reaction. In enzyme assay, the o-dianisidine coupled reaction method was used. The assay mixture contained 2.5 mM–35 mM substrate, 0.24 mg/ml o-dianisidine, 8 unit/ml horseradish peroxidase, 0.2 μM FAD and 50 mM sodium/potassium phosphate pH 8.2. All processes of *Bc*GO activity were performed at room temperature. Reduced o-dianisidine is colorless and oxidized one by peroxidase is colored brown. Using this properties, the oxidized o-dianisine was measured spectrophotometrically at 440 nm ($\varepsilon = 13000\ M^{-1}cm^{-1}$) [18,19].

2.3. Site-directed mutagenesis of BcGO

Site-specific mutations were created using the QuikChange site-

directed mutagenesis kit (Stratagene) and sequencing was performed to confirm the correct incorporation of mutations. Mutant proteins were purified in the same manner as the wild-type. The assay of Glycine was performed at 10 mM concentration. The reaction condition and method of *Bc*GO was the same as for the kinetics.

2.4. Crystallization of BcGO

After the purification of *Bc*GO, We crystallized the purified *Bc*GO protein using commercially available sparse-matrix screening kits (Rigaku Reagents and Molecular Dimensions). Each experiment consisted of mixing 1.0 μL of protein solution (32 mg mL^{-1} in 40 mM Tris-HCl, pH 8) with 1.0 μL of reservoir solution and equilibrating the drop against 50 μL of reservoir solution. *Bc*GO crystals were observed in several crystallization screening conditions. The best diffracting crystals appeared on day 2 using a reservoir solution consisting of 15% (v/v) tacsimate pH 7.0, 0.1 M HEPES pH 6.5, 6%(w/v) PEG 3350.

2.5. Data collection and structure determination of BcGO

The data were collected at the 7A beamline of the Pohang Accelerator Laboratory (PAL, Pohang, Korea) with a Quantum 270 CCD detector (ADSC, USA). All data were then indexed, integrated, and scaled together using the HKL2000 software package [20]. The *Bc*GO crystals belonged to $C222_1$ with unit cell parameters a = 82.18 Å, b = 132.81 Å, c = 165.21 Å, α = 90°, β = 90°, γ = 90°. Assuming two molecules of *Bc*GO per asymmetric unit, the crystal volume per unit of protein mass was 2.74 $Å^3$ Da^{-1}, which corresponds to a solvent content of approximately 55.82%. The structures of *Bc*GO were determined by molecular replacement with the CCP4 version of MOLREP using the structure of GO from *G. kaustophilus* HTA426 (PDB code 4YSH) as a search model. Model building was performed using the program WinCoot [21] and refinement was performed with CCP4 refmac5 [22]. The refined structure was deposited in the protein data bank under the PDB code 7CYX.

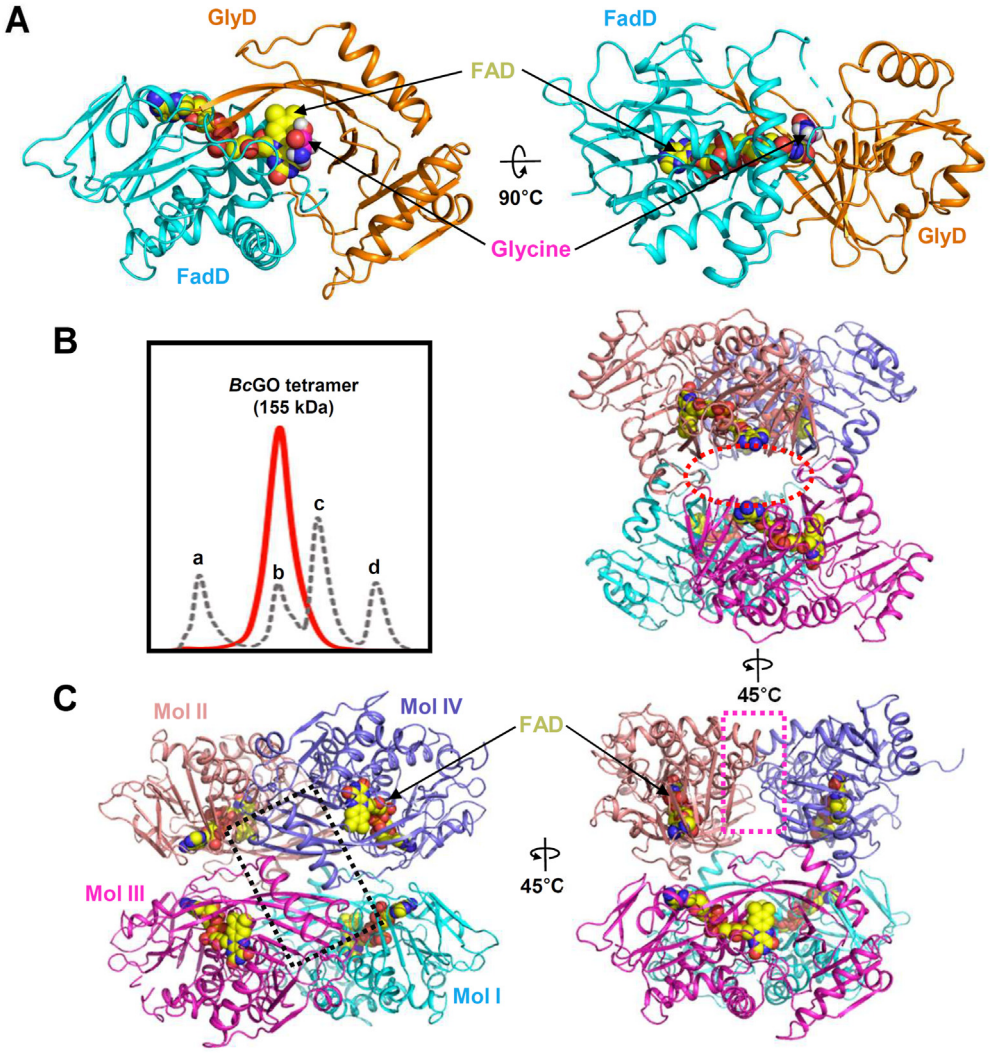

Fig. 2. Overall structure of *Bc*GO. (A) Monomeric structure of *Bc*GO. The monomeric structure of *Bc*GO is shown as a cartoon diagram, two domains are distinguished with different colors. The FAD and glycine molecules are shown as a sphere model with colors of yellow and magenta, respectively. (B) Size-exclusion chromatography of *Bc*GO. (a–d) indicate the standard samples of thyroglobulin (669 kDa), aldolase (158 kDa), conalbumin (75 kDa) and carbonic anhydrase (29 kDa). (C) Tetrameric structure of *Bc*GO. Molecules I– IV are distinguished by different color schemes. The black-colored dotted-box indicates the dimerization interface between two GlyDs. The pink-colored dotted-box indicates tetramerization interface between two FadD, and the red-colored dotted-circle indicates the large hole at the center of the *Bc*GO tetramer. (For interpretation of the references to color in this figure legend, the reader is referred to the Web version of this article.)

2.6. Molecular docking calculation

Molecular docking calculations of the glycine molecule to the *Bc*GO structure were carried out using the AutoDock Vina program. The glycine molecule was prepared using the ligand builder of WinCoot, and Prodrog in CCP4. Nonpolar H atoms were merged onto the ligands and the target protein receptor using AutoDockTools 1.5.6 prior to performing the docking calculations. For the generation of pdbqt files for both rigid and flexible receptor, flexible residues (Tyr252, and Val52 of *Bc*GO) were selected, and the bonds in the side chain of the residues were allowed to rotate. The grid box for *Bc*GO was centered at x: 62.493, y: 14.665 and z: 31.065 with sizes of 24.0, 24.0, and 20.0 Å, respectively. Nine output poses were generated with their free energy of binding calculated from its own scoring function. The final poses of glycine docked into *Bc*GO were selected based on an isoalloxazine ring moiety site of *Bc*GO and substrate binding site of *Gk*GO. The affinity of predicted docking result is −3.8 kcal/mol.

3. Results and discussion

3.1. Kinetic properties of BcGO

To investigate the biochemical properties of the glycine oxidase (BC0747) of *B. cereus* ATCC14579 strain (*Bc*GO), we overexpressed and purified the *Bc*GO protein. To investigate the enzymatic properties and stereospecificity of *Bc*GO, we measured the enzymatic activities of the protein using glycine and several L- and D-forms of small amino acids, such as D-proline and D-alanine, as substrates. We observed oxidase activity when glycine, D-proline, and D-alanine were used as substrates, whereas we did not detect any activity for L-proline and L-alanine. These results indicate that the gene product of *BC0747*, annotated as a glycine oxidase, might function as a D-amino acid oxidase. Although *Bc*GO can utilize D-amino acid as a substrate, the enzyme activities differ depending on the D-amino acid substrate used. The reactions with D-proline and D-alanine showed 77.8% and 22.7% activity, respectively, compared with the glycine reaction (Fig. 1B).

We then measured the kinetic parameters for the glycine, D-proline, and D-alanine substrates: the K_m values were 9.67, 8.58, and 45.54 mM and the apparent k_{cat} values were 2.16, 1.69, and 1.40 min^{-1} for glycine, D-proline, and D-alanine, respectively (Fig. 1C–E). These results indicate that the high activity for glycine was mainly due to the high k_{cat} value and the low activity for D-alanine was due to the high K_m value.

3.2. Overall structure of BcGO

To elucidate the molecular mechanisms of *Bc*GO, we determined its crystal structure at a 2.36 Å resolution (Supplementary Table 1). *Bc*GO showed an overall folding structure similar to GOs from *B. subtilis* (*Bs*GO, PDB code: 1RYI) [23] and *G. kaustophilus* (*Gk*GO, PDB code: 4YSH) with several regional differences. The *Bc*GO monomer is composed of 11 α-helices and 17 β-strands and can be divided into two distinctive domains: a FAD-binding domain (FadD; Met1-Ile89, Ala155-Gly224, and Asn312-Val369) and a glycine-binding domain (GlyD; Gly90-Ile154 and Thr225-Ser311) (Fig. 2A). FadD shows three-layer (ββα) sandwich fold; two β-sheets with three and six β-strands are located at one side of the domain and seven α-helices are at the other side of the domain. Although the folding of FadD is distinguishable from the three-layer sandwich fold (αβα) found in the Rossmann fold [24,25], *Bc*GO also has a conserved βαβ motif (β1, α1, and β2) for binding the dinucleotide-moiety of FAD (Fig. 2A). GlyD consists of four α-helices and an eight-stranded β-sheet, and it forms a two-layer sandwich fold, which is highly conserved in other members of the D-amino acid oxidase superfamily (Fig. 2A).

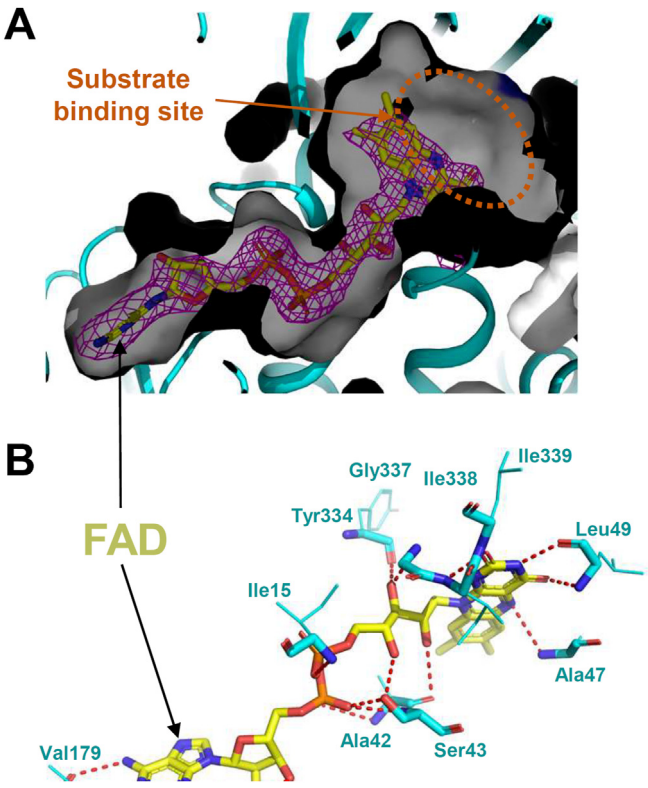

Fig. 3. Active site of *Bc*GO. (A) Electron density map of the bound FAD. The Fo-Fc electron density map of FAD is shown with magenta-colored mesh with 2.0 σ contour, and FAD is shown as a stick model with a yellow color. *Bc*GO is shown as a cartoon with cyan-colored and gray pocket formed at the center of the FadD has the FAD molecule which is tightly bound. The orange-colored dotted circle indicates a space for substrate binding. (B) FAD binding mode of *Bc*GO. FAD is shown as a stick model with a yellow color and the residues involved in the FAD binding are shown as a cyan stick model. The red-colored dotted-lines indicate hydrogen contacts between FAD molecules and *Bc*GO. (For interpretation of the references to color in this figure legend, the reader is referred to the Web version of this article.)

Although there are two *Bc*GO molecules in the asymmetric unit of the current structure, a tetrameric structure can be easily generated by $C222_1$ crystallographic symmetry operations. However, when we calculated the oligomeric status of *Bc*GO using the PDBe PISA web software, it showed that the protein forms a dimer and the tetramerization is generated by crystal contact. Thus, to investigate the oligomeric status of the enzyme, we performed size-exclusion chromatography, and *Bc*GO eluted with a molecular weight of approximately 155 kDa, suggesting that *Bc*GO exists as a tetramer in solution (Fig. 2B). The dimerization of *Bc*GO is mainly mediated via contact between two GlyDs of two molecules. In particular, the α8 and α9 helices of GlyD from one molecule (Mol 1) form a strong connection with those of the other molecule (Mol II). The side-chains of Gln 277, Thr 282, and Tyr289 and the main chains of Val 276, Glu279, Lys 296, Glu 297, and Trp 300 form a hydrogen bond network during the formation of a dimer (Fig. 2C). As calculated by PISA, the contact involved in tetramerization does not seem to be strong, and a weak connection between two FadDs from Mol I and Mol III (or Mol II and Mol IV) contributes to the tetramerization (Fig. 2C). Because of the weak interactions involved in tetramerization, we observed a large hole at the center of the *Bc*GO tetramer (Fig. 2C).

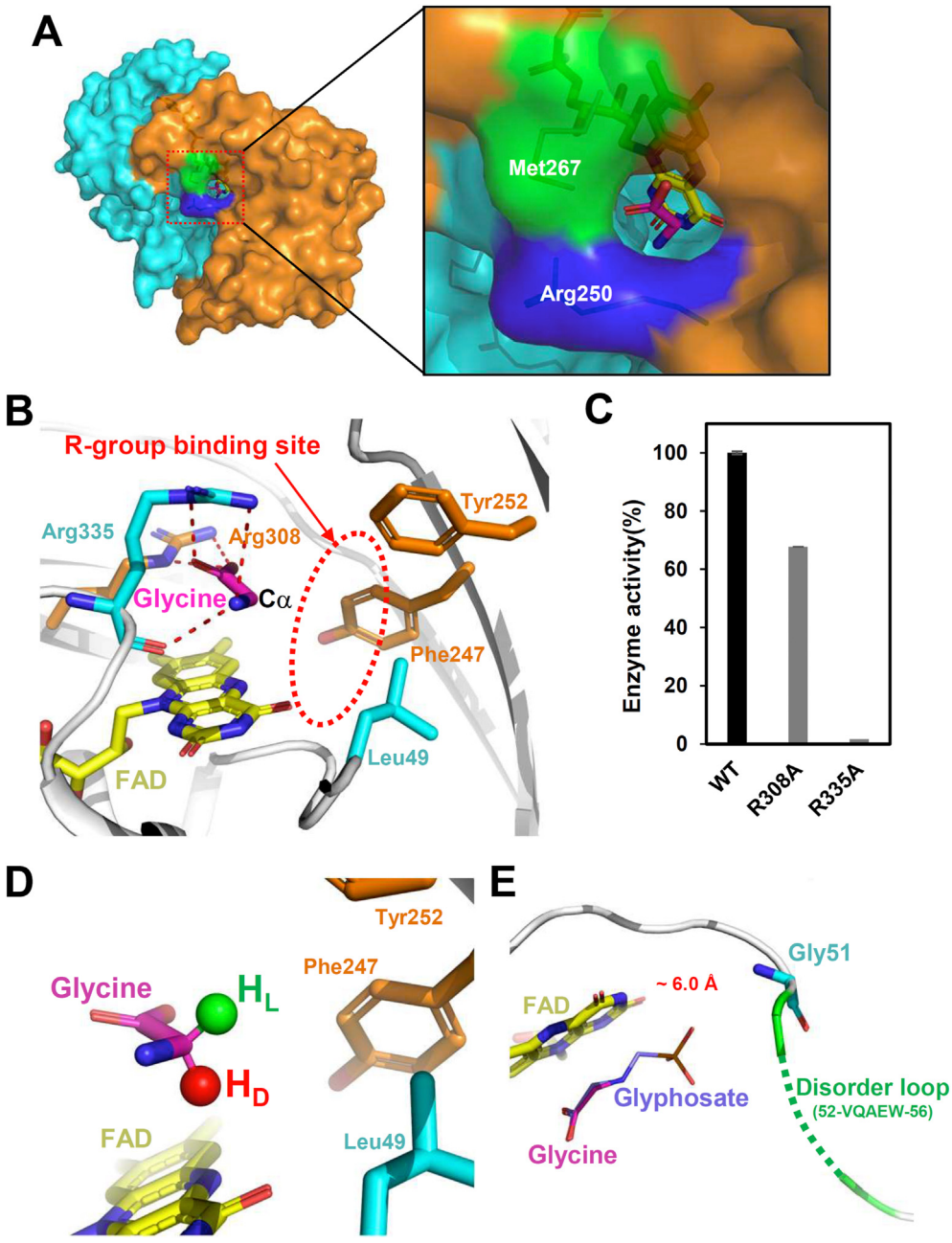

Fig. 4. Glycine and glyphosate binding mode of *Bc*GO. (A) A surface model of *Bc*GO. The *Bc*GO structure is shown as a surface model, and two domains are distinguished with a cyan and an orange colors for FadD and GlyD, respectively. Met267 and Arg 250 positioned at the entrance of the pocket are highlighted with colors of green and blue, respectively. Glycine and FAD are presented with a stick model with colors of magenta and yellow, respectively. (B) Glycine binding mode of *Bc*GO. The *Bc*GO structure is presented with a cartoon. FAD and glycine are shown as a stick model with a yellow and a magenta color, respectively. The residues from FadD and GlyD are colored by a cyan and an orange, respectively. The red-dotted-lines indicates the interaction between residues of *Bc*GO and Cα of glycine and the red-dotted-circle indicates the R-group binding site. (C) Site-directed mutagenesis experiments. Each experiment was performed in triplicate. (D) Stereospecificity of *Bc*GO. Hydrogen of the D-amino acid (H_D) and that of the L-amino acid (H_L) is shown as a sphere model with colors of red and green, respectively. Others are presented with a cartoon diagram with the same color scheme as in (B). (E) Glyphosate binding site of *Bc*GO. Disordered loop is shown as a green dotted-line. Glycine and glyphosate are shown as a line with colors of magenta and purple. Gly51 is shown as a cyan stick model. (For interpretation of the references to color in this figure legend, the reader is referred to the Web version of this article.)

3.3. Active site of BcGO

Although we did not add any additional FAD during the purification and crystallization procedures, we observed the FAD cofactor bound in our current *Bc*GO structure, which led us to identify the FAD-binding mode. The FAD-binding site is formed solely by one polypeptide, and each *Bc*GO monomer contains one site. The FAD molecule is tightly bound to the deep pocket formed at the center of the FadD domain, and we speculated that the binding of FAD to *Bc*GO might be crucial for the correct folding of the protein. However, we did not observe empty space around the bound FAD; because of the tight binding of FAD, we only observed a large space for substrate binding in the vicinity of the isoalloxazine ring (Fig. 3A). Both hydrophobic and hydrophilic interactions are involved in FAD-binding. For stabilization of the riboflavin-moiety, the main-chains of several amino acids, such as Ala47, Leu49,

Tyr334, Gly337, Ile338, and Leu339, form hydrogen bonds with the moiety (Fig. 3B). In particular, the residues Tyr334, Gly337, Ile338, and Leu339 are located at the GHYRNGIL loop, which is highly conserved in the bacterial GOs for FAD-binding. The diphosphate-moiety is stabilized by the main-chains of Ile15, Ala42, and Ser43 and a side-chain of Ser43 through hydrogen bonds (Fig. 3B). For stabilization of the AMP-moiety, the Glu34 residue forms a hydrogen bond with 2′- and 3′-hydroxyl groups of the ribose ring, and the main-chains of Lys35, Glu178, and Val179 form hydrogen bonds with adenine bases (Fig. 3B). Interestingly, most of the residues involved in FAD binding use their main-chains for hydrogen bonding, except for the two residues, Glu34 and Ser43, which use their side-chains.

3.4. Glycine binding mode of BcGO

To investigate the substrate-binding mode of *Bc*GO, we attempted to determine the complexed structure with the glycine substrate, but both the co-crystallization and the soaking experiments failed. As an alternative, we performed a molecular docking calculation for the binding of glycine with the putative substrate-binding site. The glycine molecule is located at the interface between the FadD and GlyD domains in the vicinity of the isoalloxazine ring of FAD. In our current structure, the entrance of the substrate-binding pocket is so narrow that the D-amino acid substrates cannot enter into the pocket. We observed that two residues, Arg250 and Met267, are positioned at the entrance of the pocket, and these two residues do not interact with other neighboring residues (Fig. 4A). Based on these observations, we proposed that a conformational change enlarges the entrance of the substrate-binding pocket to allow the substrates to enter, and this conformational change may occur at the Agr250 and/or Met267 residues. The carboxyl group of glycine is stabilized by two arginine residues, Arg308 and Arg335, through a hydrogen bond and a salt bridge, and the amine group is connected to both the side-chain and main-chain of Arg335 through a salt bridge and hydrogen bond, respectively (Fig. 4B). To verify the involvement of these two arginine residues in the stabilization of the glycine substrate, we replaced these residues with alanine and measured the oxidase activity of the variants. Interestingly, the *Bc*GO with Arg308 mutated to alanine (*Bc*GO^{R308A}) variant showed 67% activity compared with wild type of *Bc*GO (*Bc*GO^{WT}), while the *Bc*GO with Arg335 mutated to alanine (*Bc*GO^{R335A}) variant exhibited almost complete loss of activity (Fig. 4C). We believe that the activity loss of the *Bc*GO^{R335A} variant seems to be due to the involvement of the Arg335 residue in the stabilization of both the amine and the carboxyl group of the glycine. However, in the *Bc*GO^{R308A} variant, the Arg335 residue still formed a hydrogen bond with the carboxyl group and, consequently, contributes to a significant amount of activity.

Based on the orientation of the calculated glycine molecule, we predicted the binding site for the R-group of the D-amino acid substrates. The residues Leu49, Phe247, and Tyr252 are located at the side facing the R-group, and we speculated that these three residues may be involved in the formation of the R-group-binding site. These observations can also provide the structural basis for the stereospecificity of *Bc*GO. If a D-form amino acid binds to the substrate-binding site, the hydrogen of the D-amino acid (H_D) is directed toward the isoalloxazine ring of FAD, which enables enzyme catalysis. On the other hand, when the L-amino acid enters the substrate-binding site, the hydrogen of the L-amino acid (H_L) is on the opposite side of the isoalloxazine ring, disabling enzyme catalysis (Fig. 4D).

3.5. Structural basis for enhanced activity of glyphosate

The *Bc*GO variant with nine point mutations has been reported to show a dramatic increase in activity against glyphosate with a Km value of 1/160 compared with WT, and, specifically, the replacement of Gly51 by arginine is one of the key reasons for the enhanced activity [14]. In addition, the structural explanation of the enhanced activity resulting from the G51R mutation was provided by the docking calculation for the glyphosate molecule into the simulated *Bc*GO structure [14]. Because the crystal structure was available, we attempted to ascertain the structural basis for the enhancement of activity resulting from the G51R mutation. When we placed the glyphosate molecule at the substrate-binding site by paring the glycine-moiety of glyphosate with the glycine molecule, the phosphate-moiety of glyphosate was directed to the Gly51 residue. We suspected that the mutated arginine residue may be involved in the stabilization of the phosphate-moiety of glyphosate through a salt bridge. Interestingly, the loop where Gly51 is located, is highly disordered, and we also suspected that the loop might be stabilized by the binding of glyphosate.

In summary, we concluded that the gene product of *BC0747* from the *B. cereus* strain ATCC14579, which is annotated as a glycine oxidase (*Bc*GO), may function as a D-amino acid oxidase. We also determined the crystal structure of *Bc*GO complex with the FAD cofactor. Through the docking calculation for the glycine molecule, we identified how the carboxyl and amine groups of the D-amino acid are stabilized, and we suggested the structural basis for the enzyme's stereospecificity to D-amino acids. Additionally, our structural studies demonstrated how the mutation of Gly51 to arginine leads to a more optimized binding site for the glyphosate molecule.

Declaration of competing interest

The authors declare that they have no known competing financial interests or personal relationships that could have appeared to influence the work reported in this paper.

Acknowledgements

This work was supported by Cooperative Research Program for Agricultural Science & Technology Development (Project No. PJ01492602), Rural Development Administration, Republic of Korea.

Appendix A. Supplementary data

Supplementary data to this article can be found online at https://doi.org/10.1016/j.bbrc.2020.09.093.

References

[1] Y. Nishiya, T. Imanaka, Purification and characterization of a novel glycine oxidase from Bacillus subtilis, FEBS Lett. 438 (3) (1998) 263–266.
[2] M.Y. Equar, Y. Tani, H. Mihara, Purification and properties of Glycine oxidase from Pseudomonas putida KT2440, J. Nutr. Sci. Vitaminol. 61 (6) (2015) 506–510.
[3] I. Martinez-Martinez, et al., Characterization and structural modeling of a novel thermostable glycine oxidase from Geobacillus kaustophilus HTA426, Proteins 70 (4) (2008) 1429–1441.
[4] K. Zhang, et al., Characterization and directed evolution of BliGO, a novel glycine oxidase from Bacillus licheniformis, Enzym. Microb. Technol. 85 (2016) 12–18.
[5] V. Job, et al., Overexpression of a recombinant wild-type and His-tagged Bacillus subtilis glycine oxidase in Escherichia coli, Eur. J. Biochem. 269 (5) (2002) 1456–1463.
[6] F. Jamil, et al., Mechanistic and stereochemical studies of glycine oxidase from

Bacillus subtilis strain R5, Biochemistry 49 (34) (2010) 7377–7383.
[7] G. Molla, et al., Kinetic mechanisms of glycine oxidase from Bacillus subtilis, Eur. J. Biochem. 270 (7) (2003) 1474–1482.
[8] C.T. Jurgenson, T.P. Begley, S.E. Ealick, The structural and biochemical foundations of thiamin biosynthesis, Annu. Rev. Biochem. 78 (2009) 569–603.
[9] E.C. Settembre, et al., Structural and mechanistic studies on ThiO, a glycine oxidase essential for thiamin biosynthesis in Bacillus subtilis, Biochemistry 42 (10) (2003) 2971–2981.
[10] E. Rosini, et al., Novel biosensors based on optimized glycine oxidase, FEBS J. 281 (15) (2014) 3460–3472.
[11] A. Nicolia, et al., Expression of an evolved engineered variant of a bacterial glycine oxidase leads to glyphosate resistance in alfalfa, J. Biotechnol. 184 (2014) 201–208.
[12] M. Pedotti, et al., Glyphosate resistance by engineering the flavoenzyme glycine oxidase, J. Biol. Chem. 284 (52) (2009) 36415–36423.
[13] P. Yao, et al., Improvement of glycine oxidase by DNA shuffling, and site-saturation mutagenesis of F247 residue, Int. J. Biol. Macromol. 79 (2015) 965–970.
[14] T. Zhan, et al., Improving glyphosate oxidation activity of glycine oxidase from Bacillus cereus by directed evolution, PloS One 8 (11) (2013), e79175.
[15] G.B. Wu, et al., Asn336 is involved in the substrate affinity of glycine oxidase from Bacillus cereus, Electron. J. Biotechnol. 22 (2016) 26–30.
[16] N. Ivanova, et al., Genome sequence of Bacillus cereus and comparative analysis with Bacillus anthracis, Nature 423 (6935) (2003) 87–91.
[17] M. Kanehisa, S. Goto, KEGG: Kyoto Encyclopedia of genes and genomes, Nucleic Acids Res. 28 (1) (2000) 27–30.
[18] L.J. Chlumsky, et al., Preparation and properties of recombinant corynebacterial sarcosine oxidase: evidence for posttranslational modification during turnover with sarcosine, Biochemistry 32 (41) (1993) 11132–11142.
[19] V. Job, et al., Glycine oxidase from Bacillus subtilis. Characterization of a new flavoprotein, J. Biol. Chem. 277 (9) (2002) 6985–6993.
[20] Z. Otwinowski, W. Minor, Processing of X-ray diffraction data collected in oscillation mode, Methods Enzymol. 276 (1997) 307–326.
[21] P. Emsley, K. Cowtan, Coot: model-building tools for molecular graphics, Acta Crystallogr D Biol Crystallogr 60 (Pt 12 Pt 1) (2004) 2126–2132.
[22] G.N. Murshudov, et al., REFMAC5 for the refinement of macromolecular crystal structures, Acta Crystallogr D Biol Crystallogr 67 (Pt 4) (2011) 355–367.
[23] M. Mortl, et al., Structure-function correlation in glycine oxidase from Bacillus subtilis, J. Biol. Chem. 279 (28) (2004) 29718–29727.
[24] I. Hanukoglu, Proteopedia: Rossmann fold: a beta-alpha-beta fold at dinucleotide binding sites, Biochem. Mol. Biol. Educ. 43 (3) (2015) 206–209.
[25] D.M. Rajathei, S. Parthasarathy, S. Selvaraj, Identification and analysis of long repeats of proteins at the domain level, Front Bioeng Biotechnol 7 (2019) 250.